Accepted Manuscript

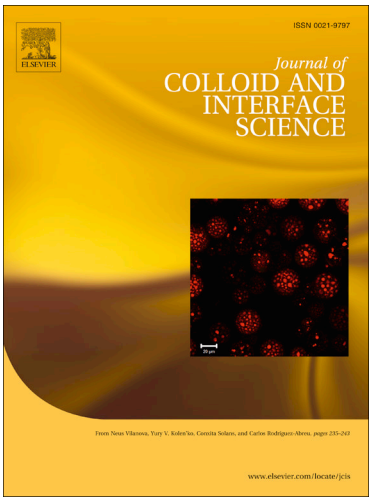

Surface nanobubbles on the rare earth fluorcarbonate mineral synchysite

Camilla L. Owens, Edgar Schach, Thomas Heinig, Martin Rudolph, Geoffrey R. Nash

PII: S0021-9797(19)30552-1
DOI: https://doi.org/10.1016/j.jcis.2019.05.014
Reference: YJCIS 24943

To appear in: *Journal of Colloid and Interface Science*

Received Date: 8 March 2019
Revised Date: 3 May 2019
Accepted Date: 4 May 2019

Please cite this article as: C.L. Owens, E. Schach, T. Heinig, M. Rudolph, G.R. Nash, Surface nanobubbles on the rare earth fluorcarbonate mineral synchysite, *Journal of Colloid and Interface Science* (2019), doi: https://doi.org/10.1016/j.jcis.2019.05.014

Title

Surface nanobubbles on the rare earth fluorcarbonate mineral synchysite

Authors

Camilla L. Owens[a*], Edgar Schach[b], Thomas Heinig[b], Martin Rudolph[b] and Geoffrey R. Nash[a]

Author affiliations

[a]*College of Engineering, Mathematics and Physical Sciences, University of Exeter, EX4 4QF, United Kingdom.*

[b]*Helmholtz Institute Freiberg for Resource Technology, Helmholtz-Zentrum Dresden-Rossendorf, Chemnitzer Staße 40, 09559 Freiberg, Germany.*

Author contact emails

Camilla Louise Owens email: co308@exeter.ac.uk

Edgar Schach email: schach32@hzdr.de

Thomas Heinig email: t.heinig@hzdr.de

Martin Rudolph email: m.rudolph@hzdr.de

Geoffrey R. Nash email: g.r.nash@exeter.ac.uk

Corresponding author

Camilla Louise Owens, University of Exeter

Email: co308@exeter.ac.uk,

Telephone: 01392 724049

Address: *College of Engineering, Mathematics and Physical Sciences, University of Exeter, EX4 4QF, United Kingdom.*

Surface nanobubbles on the rare earth fluorcarbonate mineral synchysite

Camilla L. Owens[a*], Edgar Schach[b], Thomas Heinig[b], Martin Rudolph[b] and Geoffrey R. Nash[a]

[a] *College of Engineering, Mathematics and Physical Sciences, University of Exeter, EX4 4QF, United Kingdom.*

[b]*Helmholtz Institute Freiberg for Resource Technology, Helmholtz-Zentrum Dresden-Rossendorf, Chemnitzer Staße 40, 09559 Freiberg, Germany*

*corresponding author C.L. Owens: co308@exeter.ac.uk, telephone:01392 724049

Abstract

Surface nanobubbles have been identified to play an important role in a range of industries from mineral processing to food science. The formation of surface nanobubbles is of importance for mineral processing in the extraction of complex ores, such as those containing rare earth elements. This is due to the way minerals are extracted utilising froth flotation. In this study, surface nanobubbles were imaged using non-contact atomic force microscopy on a polished cross section containing rare earth minerals. Nanobubbles were found on synchysite under reagent conditions expected to induce hydrophobicity in rare earth minerals, which is required for efficient processing.

Synchysite –(Ce) is a rare earth fluorcarbonate mineral containing over 30% rare earth elements. Relatively little research has been conducted on synchysite, with only a few papers on its surface behaviour and flotation. The resulting nanobubbles were analysed and showed an average contact angle of 24 degrees± 8. These are in line with contact angles found on dolomite and galena by previous studies.

Graphical Abstract

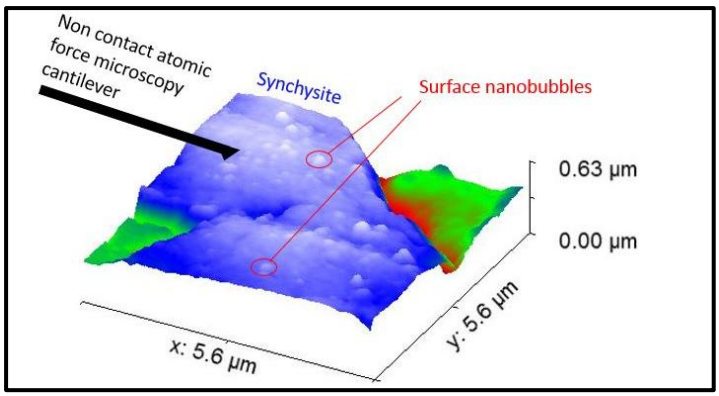

Keywords: non-contact atomic force microscopy, synchysite, bastnäsite, rare earth elements, fluorcarbonate, surface nanobubbles, carbonatite.

1. Introduction

Nanobubbles are tiny gaseous bubbles on the surface of hydrophobic materials. They have unusual properties including very small contact angles compared to macroscopic bubbles and extremely long lifetimes [1]. Since being first imaged in 2000, the use of surface nanobubbles has been explored in a wide range of industries from food to mineral processing [2-6].

Recent challenges in mineral processing include the processing of finely grained complex ores for minerals containing key materials such as rare earth elements [7, 8], sulphides [9, 10] and oxides [11]. As more conventional deposits and easily accessible ore bodies are exhausted, new deposits containing more unusual, less researched minerals are key for the future of supply of critical materials [12]. Froth flotation is the main technique of processing these ores, utilising the varying hydrophobicity of mineral surfaces under reagent regimes. Surface nanobubbles have previously been shown by Rudolph *and* Peuker [13] as a way to identify the hydrophobicity of a particle surface having a heterogeneous mineral composition. Thereby optimising flotation in complex ores of critical materials by understanding the hydrophobicity of each mineral within the ore.

Rare earth elements (REE) are a critical material identified by the European Union as vital to future development [14]. They include the fifteen lanthanide elements with the addition of scandium and yttrium [15]. The sourcing of REE has previously been

subject to fluctuation due to supply chain insecurity with new mineral sources vital for the sustainability of future supply [16-19]. Rare earth ores are highly complex, resulting in multiple stages of processing. Using life cycle analysis, the energy consumption of this extended processing effects the environmental impact of the final products they are used in such as wind turbines and electric cars [20, 21].

Synchysite- (Ce) ($CaCe(CO_3)_2$ F) is a rare earth fluorcarbonate mineral which contains over 30^{o}% (w/w) rare earth elements [22, 23]. Although not as prominent as its fluorcarbonate sibling bastnäsite, which currently supplies over 45% of the world's REE, synchysite is still economically important in a number of deposits [24-26]. It is also important as a secondary ore mineral to deposits such as Bear Lodge, Wyoming and Nechalacho, Canada [27, 28]. Understanding the effect of reagents on the surface properties of synchysite is important for optimum processing of these deposits.

The effect of mineral processing reagents on nanobubbles have previously been investigated by a selection of work, focusing on a range of minerals [29, 30]. These studies can be divided into those that focused on samples of single minerals and those that investigated complex ores [31, 32].Two studies focused on surfaces containing single minerals, Owens *et al.,* [30] focused on dolomite, a carbonate mineral, whereas Mikhlin *et al.,* [32] focused on galena, a lead sulphide mineral. Nanobubbles were found on galena under pre-treatment with oil-type collector xanthate, whereas nanobubbles were found on dolomite under depressant, surfactant-type collectors and water conditions, although nanobubble density increased under collector conditions. Previous studies on complex ores have linked nanobubbles to wettability and hydrophobicity [29, 31]. In complex ores, nanobubbles were found on eudialyte but not found on albite. Indicating nanobubbles under selective reagent regimes will form on specific minerals [13].

In this paper, we investigate surface nanobubbles on the synchysite ore under defined aqueous reagent conditions including surfactant-type collectors. Although studies have investigated complex ores [13, 29, 31], this is the first study to look at surface nanobubbles size and contact angle and to investigate nanobubbles on a rare earth fluorcarbonate mineral such as synchysite.

2. Materials & Methods

Non-contact atomic force microscopy (NC-AFM) was conducted at the Helmholtz Institute Freiberg for Resource Technology on a Park Systems (South Korea) XE100 AFM. Dynamic mode, amplitude modulated non-contact-AFM with the addition of Raman spectroscopy allowed the classification of different minerals, identifying synchysite and carbonatite gangue minerals within the ore sample. Nanobubbles were produced by the air water supersaturation method, i.e. cooling and then heating the aqueous solution to induce oversaturation. The solution was cooled to 5^{o}C and was then heated to between 30^{o}C and 40^{o}C on top of the mineral sample whilst located within the liquid cell. Collectors, used in froth flotation, including fatty acid (sodium oleate) and hydroxamic acid (AM810) in dosages and ratios favourable for bastnäsite flotation were included in the reagent mix, although the exact makeup of the aqueous solution is subject to non-disclosure. Methodology and experimental setup are the same as Owens *et al*.,[30], with the liquid cell also being used in Rudolph *and* Peuker [13, 29].

750µL of aqueous solution was added to the liquid cell by injecting with a disposable plastic nozzle attached to a pipette. Although plastic contamination has been found in nanobubble research [33, 34], this study used the same equipment and methodology as Owens *et al.,* [30] and Babel *and* Rudolph [31]. Babel *and* Rudolph [31] investigated the force curves of nanobubbles in approach and retraction showing the nanobubbles to contain gas not plastic. The same plastic injection method was also used by Ditscherlein *et al.,* [35] and Knüpfer *et al.,* [36]. The sample was cleaned between measurements by rubbing with diamond suspension [Stuers DiaPro ¼µm] before being washed with water, ethanol and water again. The sample was then sonicated before washing again with water.

The ore containing synchysite from Songwe Hill, Malawi was provided by Mkango Resources Ltd. Songwe Hill is a carbonatite deposit within the Chilwa Alkaline Province, the main ore minerals are apatite and synchysite with the main gangue minerals being ankerite and calcite. For more details of the Songwe Hill deposit geology see Al Ali [22], Broom-Fendley *et al.,* [37] and Broom-Fendley *et al.,* [38]. The mineralogy of the sample was analysed on particles in a polished epoxy resin

grain mount using Mineral Liberation Analysis (MLA) software and the SEM microscope (FEI Quanta 650 MLA-FEG machine) in combination with X-Ray spectroscopy detectors (Bruker Quantax X-Flash 5030 EDS-Detectors) in Freiberg, Germany, similar to Bachmann *et al.,* [39]. In figure 1, the mineral composition of samples from Songwe Hill, Malawi is shown, where colours refer to different mineral species. Note that the composition is not representative of the ore geology shown at Songwe Hill, please see QEMSCAN results in Al Ali [22] for more details. However, the X- Ray spectra and MLA processed images enabled the identification of the synchysite mineral investigation area within the ore sample. Raman spectroscopy was used to navigate to the location of the synchysite mineralisation. One ore section was chosen, highlighted in red, to undertake measurements of synchysite.

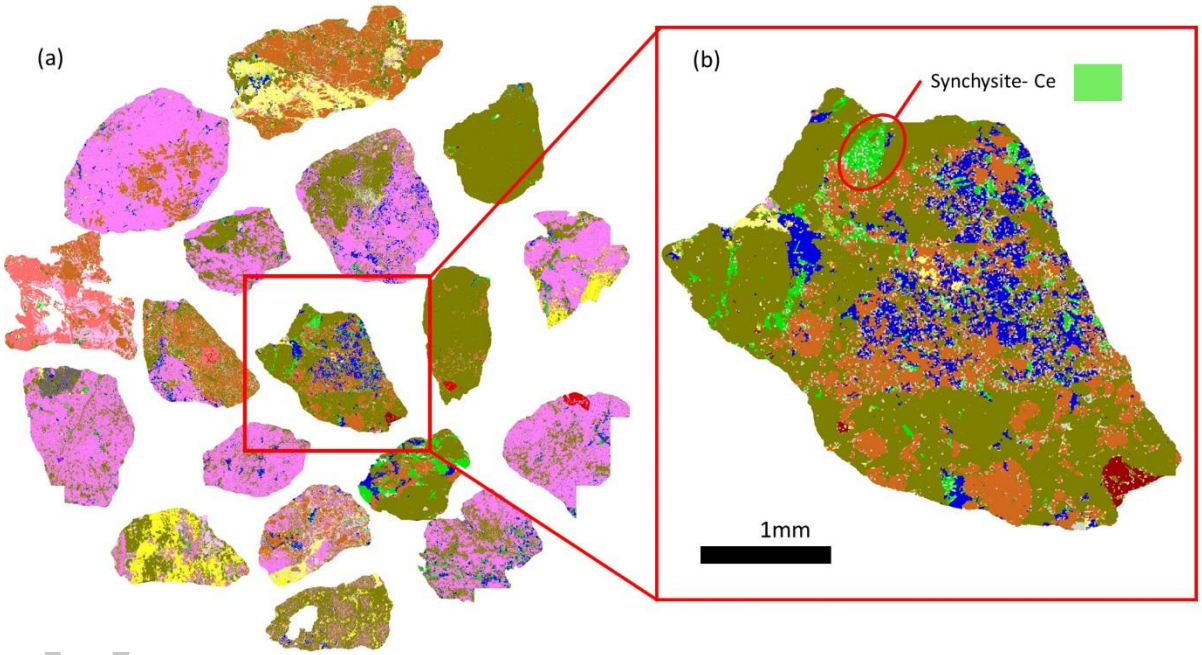

Figure 1. (a) Mineral Liberation analysis of Songwe Hill ore, light green shows synchysite, dark green is the carbonate mineral ankerite (b) Magnified area investigated in NC-AFM images. The sample area is highlighted in red.

3. Results & Discussion

In figure 2, the NC-AFM analysis of a high resolution area of 6^{o}µm x 5^{o}µm is shown. As can be clearly seen there are several small circular areas which are much higher than the surrounding topography. We identified these areas of high topography as nanobubbles by selecting bubbles over 8^{o}nm and fitting the nanobubbles to cross sections. These cross sections were fitted to the spherical cap model proposed by

Lohse *and* Zhang [40], with the effect of the cantilever tip taken into account using the methodology used in Wang *et al.,* [41] (Electronic Supplementary Information, ESI†). From spherical cap fitting, 25 nanobubbles were selected out a possible 35 nanobubble candidates (ESI†). Although the phase was not able to be clearly compared to the topography image due to the extreme topography of the sample and the surrounding phase boundaries to other minerals, there were indications that the phase changed due to the presence of nanobubbles (see ESI†). The height and lateral length of the nanobubbles were extracted from the spherical cap cross section fitted. The nanobubbles ranged in height from 71.9°nm to 14.6°nm, with their heights being much greater than the root mean square surface roughness (RMS) measured on this sample of synchysite of 1.9°nm. Although the topography over the entire measured area was much more varied with an RMS of 7.6°nm for the entire sample.

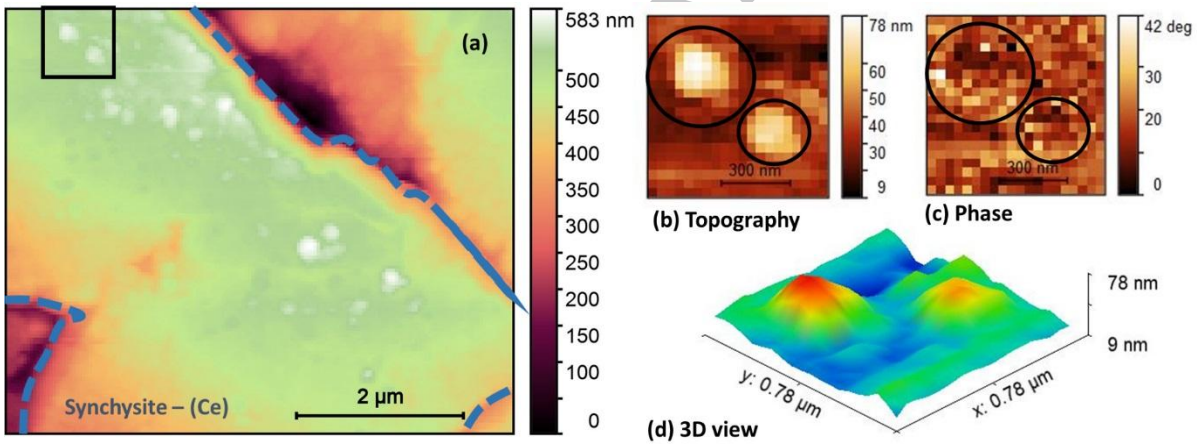

Figure 2. Nanobubbles at the surface of synchysite mineral. (a) NC-AFM image 6µm x 5µm of synchysite grain surrounded by another mineral growth from Songwe Hill, Malawi. (b) Magnified area of two nanobubbles on surface of the synchysite grain in topography, red circles highlight the two nanobubbles location (c) Phase of the two nanobubbles in (b),(d) modelled 3-D view of the nanobubbles on synchysite

The presence of nanobubbles on synchysite surface indicates that the surface was highly hydrophobic under this reagent regime. Nanobubble formation has previously been linked to reagents effecting the pinning of the nanobubbles both experimentally [30, 32] and using molecular dynamics simulations [42]. Although there are areas of extreme topography on the mineral sample, which has previously been linked to nanobubble formation, it is expected that both chemical heterogeneities, caused by

the chemical reagents, and physical heterogeneities, induce the nanobubble formation due to the pinning effects [30, 35].

The number of images acquired was affected by the extreme topography of the sample. During the cleaning protocol of rubbing with DiaPro ¼µm suspension the mineral sample had the strong possibility of splintering, causing gaps in the sample of over 30°µm. This splintering in the mineral caused extreme topography for NC-AFM imaging of holes in the sample between 50-500°nm. The splintering often caused resolution on the image to be lost. However, increased surface roughness has previously been shown to enable nanobubbles to survive under increased tapping force [35]. Future use of this technique on mineral sample needs to be aware of these problems.

The contact angle can be calculated from the height and lateral length extracted from the spherical cap fitting. The contact angle of the nanobubbles has been linked to the oversaturation within the liquid by [40]:

$$\sin(\theta) = \varepsilon \frac{P_o L}{4\sigma} = \varepsilon \frac{L}{L_c} \quad (1)$$

Θ is the contact angle of the nanobubble with ξ = oversaturation, σ = surface tension and L = length of nanobubble. With L_c (critical lateral length)= $4\sigma/P_{o\sim}$ 2.84°µm

The average contact angle of the nanobubbles measured on synchysite was 24°± 8° standard deviation. The large standard deviation in contact angle could be due to variation in line pinning highlighted by Ditscherlein *et al.,* [25] during their investigation of nanobubbles on rough alumina. The average contact angle of 23.8° was higher than previous studies of surface nanobubbles on the mineral dolomite using the same equipment and methodology, which showed a contact angle of between 15.14° and 9.74° depending on the aqueous conditions [30]. When using the typical cross sections provided by Mikhlin *et al.,* [32], the surface nanobubble contact angle on galena was 4° (10°mM collector) and 9° (0.1°mM collector), also below the values in this study. However, previous research on the silicate mineral mica has found a wide range of contact angles between 30° and 60°, demonstrating that the synchysite contact angles are not unusually high [2, 43]. The surface roughness of the synchysite was also greater than the dolomite, RMS of 1.9 nm

compared to a RMS of 1.4nm. Studies by Agrawal *et al.,* [44], and Wang *et al.,* [45], have demonstrated that physical patterning, and therefore surface roughness, can affect the location and size of nanobubbles at a surface.

Although the surface tension of macroscopic bubbles is affected by chemical reagents [46, 47], investigations into the surface tension of nanobubbles has indicated they are unaffected by reagents [48, 49]. If the surface tension is constant in nanobubbles even with the addition of reagents then oversaturation can be linked to the nanobubble contact angle using equation 1 [40]. Wang *et al.,* [41] calculated oversaturation of 8.2 using a L_c. of 2.84°µm. The same methodology was used by Owens *et al.,* [30], which showed an oversaturation of 1.7 with nanobubbles at the surface of dolomite. These results with the addition of the synchysite nanobubble data are plotted in figure 3. Using the same methodology here produces a gradient of 1.45°µm^{-1}, and therefore an oversaturation of 4.1. As the aqueous solution was heated to a higher temperature in Owens *et al.,* [30] it is expected that the oversaturation would be greater.

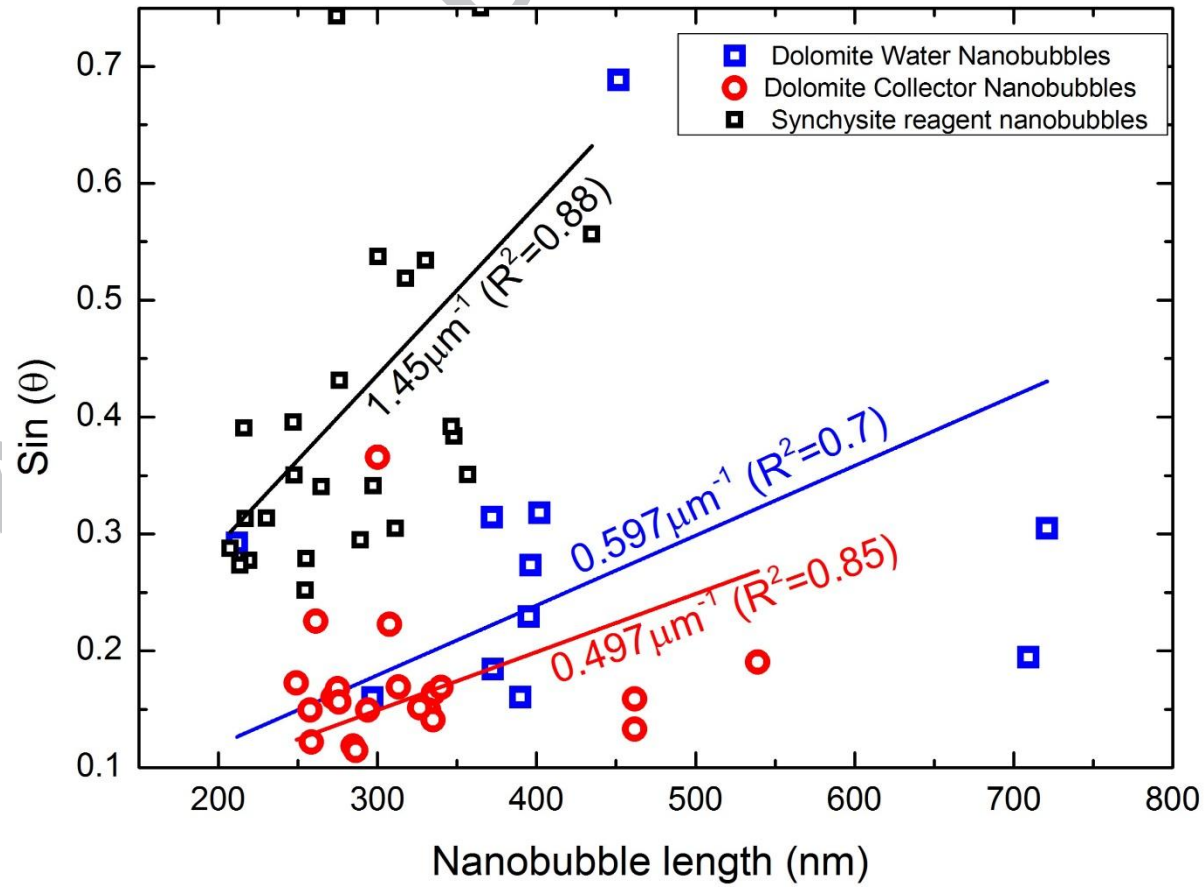

Figure 3. Nanobubble length versus sin(θ) of the contact angle. Previous results from Owens et al., [30] plotted to compare to synchysite results. Graph is plotted between 150 and 800nm and 0.1 and 0.75 sin (θ), the lines are plotted with extrapolated intersections at 0,0, using equation 1 [40].

Recent studies of bastnäsite have shown it has similar surface behaviour under flotation conditions to synchysite [50, 51]. The crystal system and calcium content of bastnäsite is different to synchysite, hexagonal with no calcium compared to monoclinic with 12% calcium [52-54]. However, similar surface behaviour is not unexpected as both synchysite and bastnäsite are rare earth fluorcarbonates with significant rare earth element concentrations, 33-43% and 63-52% respectively [50, 55]. Flotation investigations of bastnäsite ores using collectors such as hydroxamates and fatty acids have shown a high percentage recovery of bastnäsite from the ore [56]. Recent research into bastnäsite surface behaviour using zeta potential measurements and Fourier- transform infrared spectroscopy (FTIR) has found that hydroxamates bonding is heavily influenced by the metal cation on the mineral surface which chelates with the hydroxamic acid [57, 58]. When using 330mg/L benzohydroxamic acid, the recovery of dolomite in micro-flotation tests was found to hover around 20%, whereas recovery of bastnäsite climbed to 70% [57]. As synchysite behaves similarly to bastnäsite, it would not be unexpected that hydrophobicity and therefore recovery of synchysite would be high under similar collectors [50].

Nanobubbles on the surface of hydrophobic synchysite provide an extension of earlier work on nanobubbles under reagent regimes [13, 29, 31]. Future work on rare earth fluorcarbonates should focus on producing samples less prone to splintering, either through different cleaning techniques or through the production of synthetic samples. Using nanobubbles to determine hydrophobicity would be particularly applicable in ores that are highly complex with small grain sizes where micro-flotation or conventional contact angles are not feasible. These results also provide some insight into synchysite surface behaviour, a highly unstudied mineral.

4. Conclusion

In this work, we show the first results of nanobubbles in aqueous reagent regime, using anionic surfactants selectively adsorbing on the surface of a synchysite

containing mineral sample. Synchysite is a rare earth fluorcarbonate mineral, which is economically important in a broad selection of deposits, located in countries ranging from Malawi to India. However, synchysite has previously been relatively unstudied. Nanobubbles were selected on the basis of height and their fit to a spherical cap model. The average contact angle of the nanobubbles on synchysite was 24^{o}.This work builds on previous work on the size and distribution of nanobubbles at the surface of minerals under reagent regimes in order for selective hydrophobization. This adds to previous knowledge on other naturally hydrophobic surfaces such as graphite. These results are applicable for both nanobubble and rare earth processing research.

Acknowledgements

This research was conducted thanks to funding by the UK's Natural Environment Research Council SoS RARE Grant agreement no. NE/M 011429/1 and Mkango Resources Ltd. Thanks to Mkango Resources Ltd for providing the mineral sample used in this work. Work could not have been conducted without collaboration between Helmholtz Institute Freiberg for Resource Technology (HIF), Germany and SoS Rare (University of Exeter). Special thanks to Tom Leistner, Hoang Huu Duong, Nathalie Kupka and Bent Matthias Babel for their assistance at HIF. C L Owens is grateful for Lisa Ditscherlein of Technische Universität Bergakademie Freiberg for helpful and insightful discussions on the measurement of nanobubbles. Special thanks to the support provided by Professor Frances Wall, Camborne School of Mines, University of Exeter.

Original data from this publication is available via open access at the British Geological Survey National Geoscience Data Centre, United Kingdom (NGDC) [*57*].

No conflicts to declare.

References

[1] Lohse, D. and Zhang, X., 2015. Surface nanobubbles and nanodroplets. *Rev. Mod. Phys.*, *87*(3), p.981. https://doi.org/10.1103/RevModPhys.87.981

[2] Lou, S.T., Ouyang, Z.Q., Zhang, Y., Li, X.J., Hu, J., Li, M.Q. and Yang, F.J., 2000. Nanobubbles on solid surface imaged by atomic force microscopy. *J. Vac. Sci.*

Technol., B: Microelectron. Nanometer Struct.--Process., Meas., Phenom., *18*(5), pp.2573-2575. https://doi.org/10.1116/1.1289925

[3] Ishida, N., Inoue, T., Miyahara, M. and Higashitani, K., 2000. Nano bubbles on a hydrophobic surface in water observed by tapping-mode atomic force microscopy. *Langmuir*, *16*(16), pp.6377-6380. http://doi.org/10.1021/la000219r

[4] Ebina, K., Shi, K., Hirao, M., Hashimoto, J., Kawato, Y., Kaneshiro, S., Morimoto, T., Koizumi, K. and Yoshikawa, H., 2013. Oxygen and air nanobubble water solution promote the growth of plants, fishes, and mice. *PLoS One*, *8*(6), p.e65339. https://doi.org/10.1371/journal.pone.0065339

[5] Calgaroto, S., Wilberg, K.Q. and Rubio, J., 2014. On the nanobubbles interfacial properties and future applications in flotation. *Miner. Eng., 60*, pp.33-40. https://doi.org/10.1016/j.mineng.2014.02.002

[6] Alheshibri, M., Qian, J., Jehannin, M. and Craig, V.S., 2016. A history of nanobubbles. *Langmuir*, *32*(43), pp.11086-11100. http://doi.org/10.1021/acs.langmuir.6b02489

[7] Subrahmanyam, T.V. and Forssberg, K.E., 1990. Fine particles processing: shear-flocculation and carrier flotation—a review. *Int. J. Miner. Process. 30*(3-4), pp.265-286. https://doi.org/10.1016/0301-7516(90)90019-U

[8] Azizi, D. and Larachi, F., 2018. Immiscible dual ionic liquid-ionic liquid mineral separation of rare-earth minerals. *Sep. Purif. Technol., 191*, pp.340-353. https://doi.org/10.1016/j.seppur.2017.09.061

[9] Barbery G. (1986) Complex Sulphide Ores: Processing Options. In: Wills B.A., Barley R.W. (eds) Mineral Processing at a Crossroads. *NATO ASI Series (Series E: Applied Sciences*), vol 117. Springer, Dordrecht.

[10] Sousa, R., Futuro, A., Setas Pires, C. and Machado Leite, M., 2017. Froth flotation of Aljustrel sulphide complex ore. *Physicochem. Probl. Miner. Process*. *53*(2), pp.758-769. http://dx.doi.org/10.5277/ppmp170207

[11] Kern, M., Kästner, J., Tolosana-Delgado, R., Jeske, T. and Gutzmer, J., (2018). The inherent link between ore formation and geometallurgy as documented by complex tin mineralization at the Hämmerlein deposit (Erzgebirge, Germany). *Miner. Deposita*, pp.1-16. https://doi.org/10.1007/s00126-018-0832-2

[12] Jordens, A., Cheng, Y.P. and Waters, K.E., 2013. A review of the beneficiation of rare earth element bearing minerals. *Miner. Eng., 41*, pp.97-114. https://doi.org/10.1016/j.mineng.2012.10.017

[13] Rudolph, M. and Peuker, U.A., 2014. Mapping hydrophobicity combining AFM and Raman spectroscopy. *Miner. Eng.*, *66*, pp.181-190. https://doi.org/10.1016/j.mineng.2014.05.010

[14] Communication from the Commission to the European Parliament, The Council,The European Economic and Social Committee and the Committee of Regions on the 2017 list of Critical Raw Materials. Brussels, 13.9.2017.COM/2017/0490/final.

[15] Wall, F., 2014. Rare earth elements. *Critical metals handbook*, pp.312-339. https://doi.org/10.1002/9781118755341.ch13

[16] Humphries, M., 2013. Rare earth elements: The global supply chain.

[17] Goodenough, K.M., Wall, F. and Merriman, D., 2018. The rare earth elements: demand, global resources, and challenges for resourcing future generations. *Nat. Resour. Res., 27*(2), pp.201-216. http://doi.org/10.1007/s11053-017-9336-5

[18] Wall, F., Rollat, A. and Pell, R.S., 2017. Responsible sourcing of critical metals. *Elements*, *13*(5), pp.313-318. https://doi.org/10.2138/gselements.13.5.313

[19] Mancheri, N.A., Sprecher, B., Bailey, G., Ge, J. and Tukker, A., 2019. Effect of Chinese policies on rare earth supply chain resilience. *Resour., Conserv. Recycl.*, *142*, pp.101-112. https://doi.org/10.1016/j.resconrec.2018.11.017

[20] Pell, R., Wall, F. and Yan, X., 2017. Incorporating criticality into life cycle assessment for rare earth production. *Applied Earth Science - Transactions of the Institutions of Mining and Metallurgy: Section B,* 126 (2), pp.83-84. https://doi.org/10.1080/03717453.2017.1306282

[21] Navarro, J. and Zhao, F., 2014. Life-cycle assessment of the production of rare-earth elements for energy applications: a review. *Frontiers in Energy Research*, *2*, p.45. https://doi.org/10.3389/fenrg.2014.00045

[22] Al-Ali, S.H.A., 2016. (PhD Thesis) Mineralogy and mineral processing to optimise recovery of synchysite-(Ce) and apatite from carbonatite at Songwe Hill, Malawi. University of Exeter. http://hdl.handle.net/10871/28823

[23] Al-Ali, S., Wall, F., Sheridan, R., Pickles, J. and Pascoe, R., 2019. Magnetic properties of REE fluorcarbonate minerals and their implications for minerals processing. *Miner. Eng.,* 131, pp.392-397. https://doi.org/10.1016/j.mineng.2018.11.042

[24] Croll, R. Swinden, S. Hall, M. Brown, C. Beer, G. Scheepers, J. Redellinghuys, T. Wild, G. Trusler G, Mkango Resources Limited, Songwe REE Project, Malawi: *NI 43-101 Pre-feasibility Report Technical Report MSA Group* (Pty) Ltd. (2014).

[25] Bhushan S K. Geology of the Kamthai rare earth deposit. *J Geol Soc India,* 2015; 85(5) pp. 537–46.

[26] Tucker R D, Belkin HE, Schulz KJ, Peters SG, Horton F, Buttleman K, et al. A major light rare-earth element (LREE) resource in the Khanneshin carbonatite complex, southern Afghanistan*. Econ Geol.,* 2012, 107(2) pp. 197–208. https://doi.org/10.2113/econgeo.107.2.197

[27] Grammatikopoulos, T., Mercer, W. and Gunning, C., 2013. Mineralogical characterisation using QEMSCAN of the Nechalacho heavy rare earth metal deposit, Northwest Territories, Canada. *Can. Metall. Q., 52*(3), pp.265-277. https://doi.org/10.1179/1879139513Y.0000000090

[28] Andersen, A.K., Clark, J.G., Larson, P.B. and Donovan, J.J., 2017. REE fractionation, mineral speciation, and supergene enrichment of the Bear Lodge carbonatites, Wyoming, USA. *Ore Geol. Rev.*, *89*, pp.780-807. https://doi.org/10.1016/j.oregeorev.2017.06.025

[29] Rudolph, M. and Peuker, U.A., 2014. Hydrophobicity of minerals determined by atomic force microscopy–a tool for flotation research. *Chem. Ing. Tech.*, *86*(6), pp.865-873. https://doi.org/10.1002/cite.201400017

[30] Owens C L, Schach E, Rudolph M, and Nash G R. 2018, Surface nanobubbles on the carbonate mineral dolomite. *RSC Adv.,* 8, pp. 35448-35452. https://doi.org/10.1039/C8RA07952H

[31] Babel, B. and Rudolph, M., 2018. Characterizing mineral wettabilities on a microscale by colloidal probe atomic force microscopy. *Miner. Eng., 121*, pp.212-219. https://doi.org/10.1016/j.mineng.2018.02.003

[32] Mikhlin, Y.L., Karacharov, A.A. and Likhatski, M.N., 2015. Effect of adsorption of butyl xanthate on galena, PbS, and HOPG surfaces as studied by atomic force microscopy and spectroscopy and XPS. *Int. J. Miner. Process. , 144*, pp.81-89. https://doi.org/10.1016/j.minpro.2015.10.004

[33] Berkelaar, R.P., Dietrich, E., Kip, G.A., Kooij, E.S., Zandvliet, H.J. and Lohse, D., 2014. Exposing nanobubble-like objects to a degassed environment. *Soft Matter*, *10*(27), pp.4947-4955. https://doi.org/10.1039/C4SM00316K

[34] Wang, X., Zhao, B., Hu, J., Wang, S., Tai, R., Gao, X. and Zhang, L., 2017. Interfacial gas nanobubbles or oil nanodroplets? *Phys. Chem. Chem. Phys*. *19*(2), pp.1108-1114. https://doi.org/10.1039/C6CP05137E

[35] Ditscherlein, L., Fritzsche, J. and Peuker, U.A., 2016. Study of nanobubbles on hydrophilic and hydrophobic alumina surfaces. *Colloids Surf. , A,* 497, pp.242-250. https://doi.org/10.1016/j.colsurfa.2016.03.011

[36] Knüpfer P, Fritzsche J, Leistner T, Rudolph M, and Peuker U A, Investigating the removal of particles from the air/water-interface–Modelling detachment forces using an energetic approach. *Colloids Surf. , A,* 2017, 513, 215-222. https://doi.org/10.1016/j.colsurfa.2016.10.046

[37] Broom-Fendley, S., Brady, A.E., Wall, F., Gunn, G. and Dawes, W., 2017. REE minerals at the Songwe Hill carbonatite, Malawi: HREE-enrichment in late-stage apatite. *Ore Geol. Rev.,* 81, pp.23-41. https://doi.org/10.1016/j.oregeorev.2016.10.019

[38] Broom-Fendley, S., Brady, A.E., Horstwood, M.S., Woolley, A.R., Mtegha, J., Wall, F., Dawes, W. and Gunn, G., 2017. Geology, geochemistry and geochronology of the Songwe Hill carbonatite, Malawi. *J. Afr. Earth Sci.*, 134, pp.10-23. https://doi.org/10.1016/j.jafrearsci.2017.05.020

[39] Bachmann, K., Frenzel, M., Krause, J. and Gutzmer, J., 2017. Advanced identification and quantification of in-bearing minerals by scanning electron microscope-based image analysis. *Microsc. Microanal*. , 23(3), pp.527-537. https://doi.org/10.1017/S1431927617000460

[40] Lohse, D. and Zhang, X., 2015. Pinning and gas oversaturation imply stable single surface nanobubbles. *Phys. Rev. E*, *91*(3), p.031003. https://doi.org/10.1103/PhysRevE.91.031003

[41] Wang, Y., Li, X., Ren, S., Alem, H.T., Yang, L. and Lohse, D., 2017. Entrapment of interfacial nanobubbles on nano-structured surfaces. *Soft matter*, *13* (32), pp.5381-5388. https://doi.org/10.1039/C7SM01205E

[42] Xiao, Q., Liu, Y., Guo, Z., Liu, Z. and Zhang, X., 2017. How nanobubbles lose stability: Effects of surfactants. *Applied Phys. Lett.* , 111(13), p.131601. https://doi.org/10.1063/1.5000831

[43] Wang, X., Zhao, B., Ma, W., Wang, Y., Gao, X., Tai, R., Zhou, X. and Zhang, L., 2015. Interfacial nanobubbles on atomically flat substrates with different hydrophobicities. *ChemPhysChem*, *16*(5), pp.1003-1007. https://doi.org/10.1002/cphc.201402854

[44] Agrawal, A., Park, J., Ryu, D.Y., Hammond, P.T., Russell, T.P. and McKinley, G.H., 2005. Controlling the location and spatial extent of nanobubbles using hydrophobically nanopatterned surfaces. *Nano Lett.* , *5*(9), pp.1751-1756. https://doi.org/10.1021/nl051103o

[45] . Wang, L., Wang, X., Wang, L., Hu, J., Wang, C.L., Zhao, B., Zhang, X., Tai, R., He, M., Chen, L. and Zhang, L., 2017. Formation of surface nanobubbles on nanostructured substrates. *Nanoscale*, *9*(3), pp.1078-1086. https://doi.org/10.1039/c6nr06844h

[46] Atrafi A and Pawlik, M 2016. Surface tension and gas dispersion properties of fatty acid solutions, *Miner. Eng.,* 85, pp.138-147 https://doi.org/10.1016/j.mineng.2015.11.006

[47] Hauner, I.M., Deblais, A., Beattie, J.K., Kellay, H. and Bonn, D., 2017. The dynamic surface tension of water. *J Phys Chem Lett., 8*(7), pp.1599-1603.https://doi.org/10.1021/acs.jpclett.7b00267

[48] Zhang, X.H., Maeda, N. and Craig, V.S., 2006. Physical properties of nanobubbles on hydrophobic surfaces in water and aqueous solutions. *Langmuir*, *22* (11), pp.5025-5035. https://doi.org/10.1021/la0601814

[49] Ducker, W.A., 2009. Contact angle and stability of interfacial nanobubbles. *Langmuir*, *25*(16), pp.8907-8910. https://doi.org/10.1021/la902011v

[50] Owens, C.L., Nash, G.R., Hadler, K., Fitzpatrick, R.S., Anderson, C.G. and Wall, F., 2018. Zeta potentials of the rare earth element fluorcarbonate minerals focusing on bastnäsite and parisite. *Adv. Colloid Interface Sci.* 256, pp.152-162. https://doi.org/10.1016/j.cis.2018.04.009

[51] Jordens, A., Marion, C., Grammatikopoulos, T., Hart, B. and Waters, K.E., 2016. Beneficiation of the Nechalacho rare earth deposit: Flotation response using benzohydroxamic acid. *Miner. Eng., 99*, pp.158-169. https://doi.org/10.1016/j.mineng.2016.08.024

[52] Donnay, G. and Donnay, J.D.H., 1953. The crystallography of bastnaesite, parisite, roentgenite, and synchisite. *Am. Mineral.* , *38*(11-12), pp.932-963.

[53] Manfredi, T.R., 2013. [Masters Thesis] A mineralização de parisita–(Ce) associada ao carbonatito Fazenda Varela (Correia Pinto, SC).

[54] Ni, Y., Post, J.E. and Hughes, J.M., 2000. The crystal structure of parisite-(Ce), Ce2CaF2 (CO3) 3. *Am. Mineral.* ,*85* (1), pp.251-258. https://doi.org/10.2138/am-2000-0126

[55] Andersen, T., 1986. Compositional variation of some rare earth minerals from the Fen complex (Telemark, SE Norway): implications for the mobility of rare earths in a carbonatite system. *Mineral. Mag., 50*(357), pp.503-509. https://doi.org/10.1180/minmag.1986.050.357.13

[56] Yang, X., Satur, J.V., Sanematsu, K., Laukkanen, J. and Saastamoinen, T., 2015. Beneficiation studies of a complex REE ore*. Miner. Eng.*, 71, pp.55-64. https://doi.org/10.1016/j.mineng.2014.10.005

[57] Espiritu, E.R.L., Naseri, S. and Waters, K.E., 2018. Surface chemistry and flotation behavior of dolomite, monazite and bastnäsite in the presence of benzohydroxamate, sodium oleate and phosphoric acid ester collectors., *Colloids Surf., A, 546*, pp.254-265. https://doi.org/10.1016/j.colsurfa.2018.03.030

[58] Espiritu, E.R.L., da Silva, G.R., Azizi, D., Larachi, F. and Waters, K.E., 2018. The effect of dissolved mineral species on bastnäsite, monazite and dolomite flotation using benzohydroxamate collector. *Colloids Surf., A, 539*, pp.319-334. https://doi.org/10.1016/j.colsurfa.2017.12.038

[59] NC-AFM images of nanobubbles on synchysite. National Geoscience Data Centre Archive. University of Exeter, Camilla Owens. DOI. [to be added].

Graphical abstract